

# Molecularly controlled functional architectures

This paper summarizes some of our efforts in designing and synthesizing bio-functional layers at solid/solution interfaces, characterizing their structure and dynamics, and optimizing their functional properties. We explore different materials and architectures, focusing here on hydrogels and lipid bilayer membranes.

Eva-Kathrin Sinner<sup>a,b,c</sup>, Sandra Ritz<sup>a,b</sup>, Yi Wang<sup>d</sup>, Jakub Dostálek<sup>d</sup>, Ulrich Jonas<sup>e</sup>, and Wolfgang Knoll<sup>\*c,d</sup>

<sup>a</sup>Max-Planck-Institute for Polymer Research, Ackermannweg 10, 55128 Mainz, Germany

<sup>b</sup>Johannes Gutenberg University of Mainz, 55099 Mainz, Germany

<sup>c</sup>Institute of Materials Research and Engineering, 3 Research Link, Singapore

<sup>d</sup>AIT Austrian Institute of Technology, Donau-City-Strasse 1, 1220 Vienna, Austria

<sup>e</sup>FORTH/IESL - BOMCLab, Voutes Str. 100, 71110 Heraklion, Greece

E-mail: [wolfgang.knoll@ait.ac.at](mailto:wolfgang.knoll@ait.ac.at)

The design and synthesis of molecularly or supra-molecularly defined interfacial architectures have seen in recent years a remarkable growth of interest and scientific research activities for various reasons. On the one hand it is generally believed that the construction of an interactive interface between the living world of cells, tissue or whole organisms and the (inorganic or organic) materials world of technical devices, like implants or medical parts requires the proper construction and structural (and functional) control of this organism-machine interface<sup>1</sup>. We are still at the very beginning of generating a better understanding of what is needed to make an organism tolerating implants, to guarantee the bidirectional communication between microelectronic devices and living tissue or to simply construct an interactive biocompatibility of surfaces in general<sup>2</sup>.

On the other hand, the relatively simple interface between a technical transducer used in a biosensor format and the analyte solution of interest constitutes a challenge for the supra-molecularly controlled assembly of the interfacial architecture. In addition to the need to optimize the specific interaction between the binding sites at the sensor surface and the analyte from solution, one of the

major tasks for the proper design of the interfacial bio-functional architecture, actually, is the minimization of the non-specific binding of biomolecules from a physiological solution<sup>3,4</sup>. Typically, these species are by far in excess and at concentrations for which already rather weakly affine binding sites generate a significant interfacial signal interfering with that originating from the specifically bound biomolecules of interest.

The gene chip is a well-established sensor platform for the detection of oligonucleotides, PCR amplicons, generic DNA, etc., for a variety of biological and medical applications. Many questions remain to be solved associated, for example, with the fact that DNA intrinsically is a highly charged polyelectrolyte system. In a dilute bulk solution, at an interface this feature can cause all kinds of problems related, for example, to the Coulombic interactions of the surface-attached capture probes with the analyte target strands binding from solution, or the possible cross-talk between neighboring hybridization sites, to mention but a few.

Not quite the same level of maturity, however, already beyond a purely experimental stage are arrays that detect various kinds of proteins, with applications ranging from monitoring expression levels

to helping in cancer diagnostics and other disease detection. Here, the practical problems are still much more serious than in the case of the gene chip but first commercial products are appearing on the market.

And finally, a membrane chip does not exist at all; for many years it has been speculated that there has been significant activity in Australia – headed by Bruce Cornell. However, despite some interesting general scientific papers<sup>5,6</sup> no report about the successful introduction of a real product has appeared so far. Moreover, the Australian group focused on the use of gramicidin, a well-known pore-forming peptide that upon dimerization opens an ion channel through the membrane. Our approach is much more general (and allows for a broad range of potential application from binding studies in drug development addressing membrane-integral receptors, to the elucidation of membrane associated pathogenic processes like the amyloid plaque formation in the development of Alzheimer's disease<sup>7</sup>), it allows for the use of the developed platform as a 'phantom cell' for a detailed evaluation of the essential processes underlying cell-cell contact<sup>8</sup>, i.e., in cancer development or for general tissue engineering purposes, or for the development of strategies to overcome current concerns for classical antibiotics which find more and more bacterial strains resistant to the traditionally applied antibiotic drugs<sup>9</sup>.

In this paper, we will concentrate on just the biosensor aspect and focus on two architectures, i.e., the fabrication and functionalization of a hydrogel matrix used in optical bio-affinity studies of a classical target, the prostate specific antigen (PSA) and the implementation of a novel model membrane platform, the tethered lipid bilayer for the cell-free expression of membrane proteins, in particular, G-protein-coupled receptors (GPCR). The development of a variety of surface analytical tools that offer a detailed picture of the interface, and any molecular architecture that is assembled to it, has opened the window of opportunities to a much better and deeper understanding of the organization and structural characteristics of any supramolecular coating that is prepared at the interface with the aim at controlling its functional performance. Hence, in the examples for supramolecular interfacial architectures that we will discuss below we will put particular emphasis on the correlation between the requirements of the transduction principles and how one can design the surface architecture to meet these needs.

## Supramolecular interfacial architecture for bio-affinity studies

### Grafted hydrogel layers for biosensor functionalization

Our strategy for the preparation of highly swollen hydrogels is based on the synthesis of ter- (or even quarter-) polymers incorporating monomers that control the base properties of the resulting hydrogel. This includes the manipulation of its hydrophilic/hydrophobic character which influences parameters like the collapse temperature (lower critical solution temperature, LCST). Other monomers can be used for the covalent coupling of the binding partners, e.g., antigens

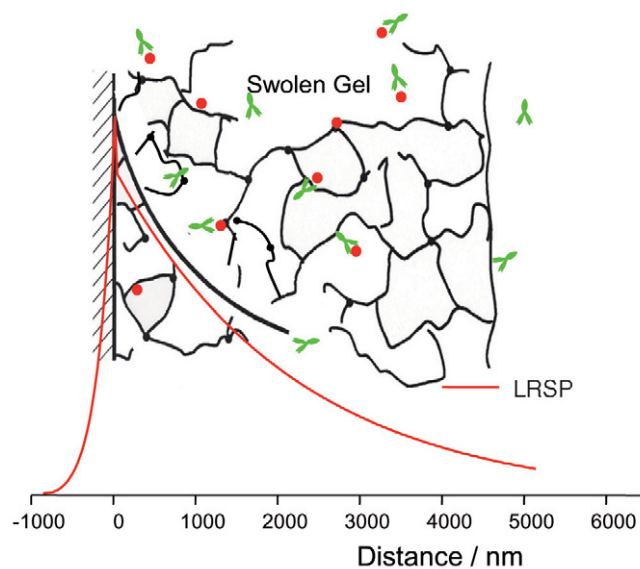


*Fig. 1 The interfacial architecture of a grafted, highly swollen hydrogel, functionalized by binding sites (red dots) to which analyte molecules from solution (green objects) can bind. For comparison, the extended electromagnetic field of a long range surface plasmon (LRSP) mode propagating along the solid/solution interface is plotted (red curve). Note that the gel as well as the evanescent field extends some micrometers into the analyte solution.*

or antibodies, organic dyes, (semiconducting or even magnetic) nanoparticles, etc. And finally, this concept includes cross-linking units which in our case function by the hydrogen abstraction properties of benzophenon units<sup>10</sup>. After spin-coating this copolymer onto a substrate, which is pre-conditioned by a self-assembled monolayer of benzophenon derivatives of long alkyl chain molecules, the benzophenon moieties are photo-activated by UV light resulting in a simultaneous cross-linking and grafting of the polymer layer to the substrate. Immersion into a buffer solution then leads to the formation of the hydrogel that can swell to a thickness that exceeds its dry value by up to a factor of 40<sup>11</sup>. This means that these matrices are very open structures allowing for an easy access of the analytes by diffusion from the bulk solution to their stationary partners inside the gel resulting in a nearly unrestricted affinity binding reaction<sup>12</sup>. This is schematically sketched in Fig. 1. Here, the swollen thickness is chosen so as to match to the evanescent tail of the optical field of a long-range surface plasmon mode (cf. below) extending also some few  $\mu\text{m}$  into the buffer medium.

### Long range surface plasmon fluorescence spectroscopy

Among the many experimental techniques well-suited for the structural and functional characterization of such interfacial architectures in contact with an aqueous phase surface plasmon resonance (SPR) spectroscopy<sup>13,14</sup> has gained an enormous popularity as an ultra sensitive optical technique<sup>15</sup>. In particular, the introduction of a

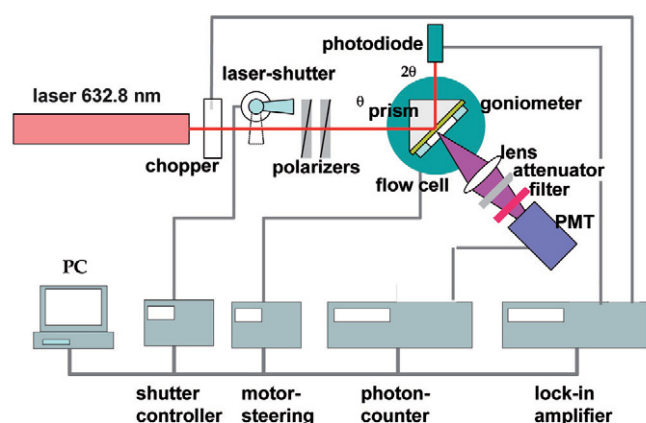


Fig. 2 Extension of a Kretschmann surface plasmon spectrometer by a fluorescence detection unit consisting of a collection lens, an attenuator (if needed), a set of filters for the separation of scattered light, and a photomultiplier tube (PMT) or a (color) CCD camera for the microscopic mode of operation.

variety of commercial instruments has helped to spread the use of the SPR technique that is now routinely used in materials research and life science laboratories. The fundamental set-up based on the Kretschmann prism coupling configuration is given in Fig. 2: onto a high-index glass prism a thin Au- or Ag- film is evaporated (functionalized by an interfacial architecture designed for a specific

bio-affinity reaction) and then brought into direct contact with the aqueous phase of the analyte solution (cf. also Fig. 3a). If a laser beam is coupled to and reflected off the metal/buffer interface via the prism the excitation of a surface plasmon mode can be seen as a sharp dip in the angular reflectivity scan. This is simulated with a Fresnel-based algorithm and shown in Fig. 3b) for the case of a 50 nm thin Ag film. One of the typical features of the excited surface plasmon mode is the evanescent character of its optical field which peaks at the interface and decays exponentially into the buffer phase. For an Au film of 40 nm and a wavelength of  $\lambda = 633$  nm the  $(1/e)$  penetration depth into the analyte solution amounts to about  $L_z = 180$  nm as it is shown in Fig. 3c.

A recently introduced extension of SPR for bio-affinity studies uses this surface-confined electromagnetic mode for the excitation of chromophores that are bound to the analyte of interest<sup>16</sup>. Upon the approach and docking of the analytes to their surface-attached binding partners (e.g., catcher probe DNA strands or an antigen) these chromophores are excited by the propagating surface plasmon mode, resulting in the emission of strong fluorescence light<sup>17</sup>.

The experimental set-up used to record this emission as a function of time, excitation angle, etc. is given in Fig. 2: a regular SPR instrument is complemented by a module consisting of a collection lens, a set of filters specific for the emitted fluorescence photons, and

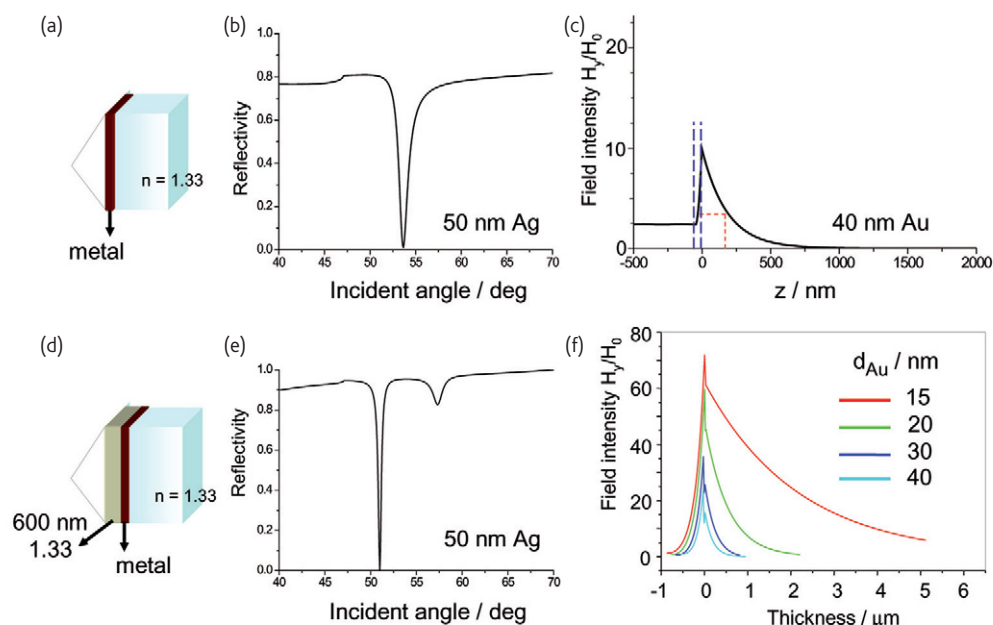


Fig. 3 (a) Schematics of the Kretschmann configuration for surface plasmon excitation; (b) angular reflectivity scan simulated for a high refractive index prism ( $n=1.85$  @  $\lambda=633$  nm, 50 nm Ag with  $\epsilon = -17. +0.7i$ , in contact with water of  $n=1.33$ ); (c) optical field distribution,  $H_y$ -versus- $z$ , normal to the interface for the architecture given in (a) but calculated for 40 nm (cf. the broken blue lines) of Au ( $\epsilon = -12.3 + 1.29i$ ) as the metal layer; (d) Kretschmann configuration for the excitation of LRSRP: onto the high index prism first a layer of a low index cladding layer is deposited (here assumed with  $n=1.33$ ), followed by the metal coating (Ag with  $d=50$  nm), operating in water; (e) reflectivity scan simulation for the architecture given in (d). Note the two minima at lower and at higher angles, respectively, relative to the parent resonance in the 'normal' SPR (cf. (b)); (f) optical field distribution for a layer architecture similar to the one given in (d), however, calculated for thin Au layers with  $\epsilon = -12.3 + 1.29i$  and varying thicknesses, as indicated, and a refractive index of the cladding layer of  $n=1.29$ . Note the substantial asymmetry in the field distribution, however, with a significantly extended decay length into the analyte solution (in order to better show this difference to normal SPR (cf. (c)) we scaled both fields to the value at the metal/water interface).



a photomultiplier. It has been shown in a series of investigations that this mode of surface plasmon fluorescence spectroscopy (SPFS) allows for a very sensitive recording of bio-affinity reactions<sup>18</sup>. Examples given in the literature include architectures based on a carboxy-dextran brush used to couple covalently the antigens as the recognition sites. The thickness of the swollen brush matched the evanescent surface plasmon field and prevented the chromophores from being quenched by the proximity to the metal substrate. This way, extreme sensitivities could be achieved<sup>19</sup>. This extension of SPR spectroscopy with fluorescence detection has been successfully applied to a number of bio-affinity studies with proteins, oligonucleotides or PCR amplicons, e.g., with discrimination of single-nucleotide polymorphism (SNP)<sup>20</sup>.

A very promising extension of using surface plasmon modes as the excitation light source in conjunction with fluorescence detection schemes is the application of long-range surface plasmons (LRSP). A general scheme based on the Kretschmann configuration for their excitation is given in Fig. 3d: prior to the noble metal deposition a cladding layer of a low refractive index material close to that of the working medium buffer ( $n \approx 1.33$ ) is coated onto the prism, thus generating a nearly symmetrical sandwich structure upon placing the sample in an aqueous medium. The evanescent optical fields of the surface plasmon modes propagating along the two metal/dielectric interfaces with (nearly) identical dispersion properties interact weakly through the metal. Thus, their degeneracy is lifted and two new modes appear in the reflectivity scan (cf. Fig. 3e), a so-called long-range and a short-range surface plasmon<sup>21</sup>. Two features of the long-range surface plasmon modes are particularly interesting in connection with fluorescence spectroscopy of analytes bound to the surface matrix.

The first advantage is the extended range of the evanescent field reaching much farther out into the buffer solution than normal surface plasmon waves (cf. Figs. 3c and f, respectively), thus allowing for the detection of fluorescence photons from a thicker slice of the sensor surface architecture. The second one is the higher optical field of the evanescent tail<sup>22</sup>, giving rise to a second mechanism for enhanced fluorescence detection<sup>23</sup>.

#### Detection of free prostate specific antigen by long range surface plasmon fluorescence spectroscopy.

The experimental platform that combines the layer architecture required for the excitation of long-range surface plasmons and the sensor binding matrix based on an antibody functionalized hydrogel are shown in Fig. 4. The base cladding layer consisting of a Teflon-like polymer material that can be simply spin-coated onto the high index glass prism is evaporation-coated by a 15–40 nm thick Au metal layer that is further functionalized by the hydrogel as the binding matrix.

For the SPFS detection of free PSA (f-PSA) in HBS-EP buffer (degassed 10 mM HEPES buffer saline, pH 7.4, 150 mM NaCl, 3 mM EDTA, 0.005% (v/v) surfactant P-20) and human serum, a photo-crosslinked dextran hydrogel with a thickness of  $d_h = 1.32 \mu\text{m}$  and a surface mass density of  $\Gamma = 56 \text{ ng mm}^{-2}$  was used<sup>24</sup>. Into the gel, the capture antibody c-Ab was immobilized with a surface mass density of  $\Gamma = 41 \text{ ng mm}^{-2}$ . In these experiments, buffer and human serum samples spiked with f-PSA were analyzed. Fig. 5 shows the time evolution of the fluorescence signal  $F$  measured during the five detection cycles for the HBS-EP samples spiked with f-PSA at concentrations of 0 – 10 pM. For the concentration of f-PSA equal

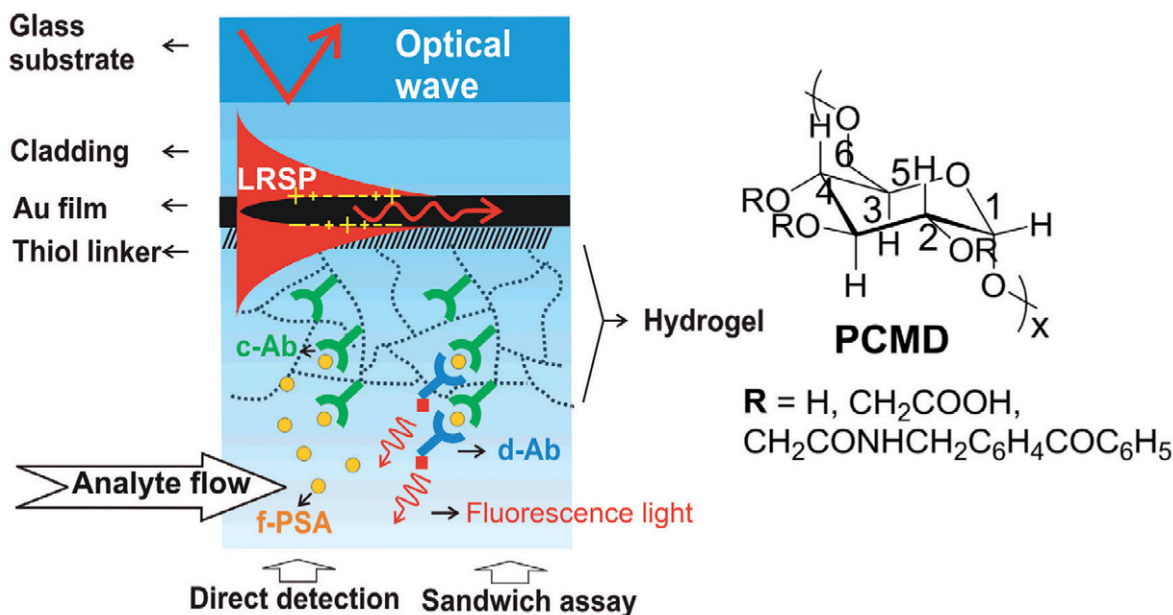


Fig. 4 Interfacial sensor architecture for the direct, label-free detection of free prostate-specific antigen (f-PSA, yellow disks) by binding to the gel-coupled capture antibodies (green symbols) via SPR, or after sandwiching by a chromophore-labeled detection antibody (blue symbols) via fluorescence detection by SPFS.

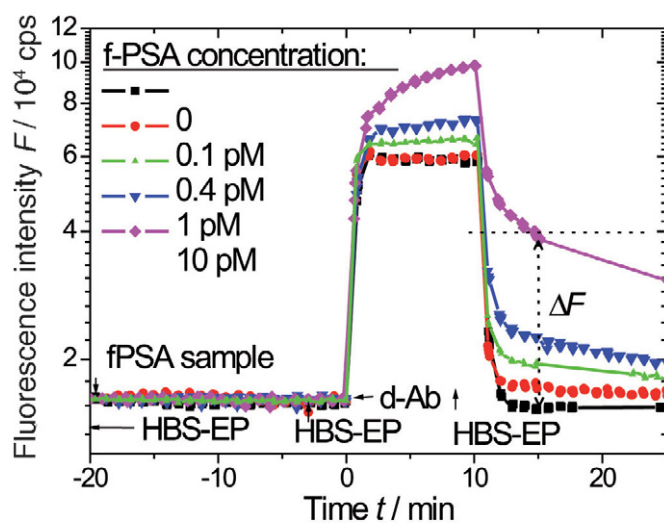


Fig. 5 Time evolution of the fluorescence signal  $F$  upon the analysis of HBS-EP samples spiked with f-PSA at concentrations 0 - 10 pM.

to zero, a rapid step-like increase and decrease in the fluorescence signal  $F$  was observed at time  $t = 0$  and 10 min, respectively, due to the diffusion of the detection antibodies (d-Ab) into and out of the gel. No measurable change in the fluorescence signal  $\Delta F$  was observed for the blank HBS-EP buffer sample, and the sample with f-PSA at a concentration of 10 pM induced a sensor response of  $\Delta F = 2.3 \times 10^4$  cps.

Similarly, we measured the sensor response  $\Delta F$  for a series of human serum samples spiked with f-PSA. For the analysis of blank human serum sample not spiked with f-PSA, a significant increase in the sensor response of  $\Delta F(0) \sim 625$  cps was observed which was probably due to the non-specific adsorption of d-Ab to the blood plasma components adhering to the sensor surface. The comparison of the calibration curve for the direct detection f-PSA in HBS-EP buffer (SPR) and for the fluorescence readout of a sandwich immunoassay detection scheme of f-PSA in HBS-EP and human serum (SPFS) is presented in Fig. 6. The limit of detection (LOD) for the SPFS readout was defined as the concentration for which the linear fit of the calibration curve intersects with that for a blank sample  $\Delta F(0)$  plus three times the standard deviation of the fluorescence signal  $3\sigma(F) = 230$  cps. For the detection in HBS-EP buffer and human serum, the LOD of 34 and 330 fM was determined, respectively. The LOD of f-PSA in human serum is about one order of magnitude higher than that of PSA in buffer probably due to slower diffusion of f-PSA into the gel in the serum which exhibit higher viscosity and owing to the blocking the c-Ab antibody immobilized in the hydrogel matrix by means of non-specific adsorption. The sensor surface showed good reproducibility with the relative standard deviation of the sensor response  $\Delta F$  of 4% after 30 detection cycles and four days of operation. SPFS-based analysis of an individual sample was performed in 30 minutes including the 15-minute incubation of the sensor surface with a sample,

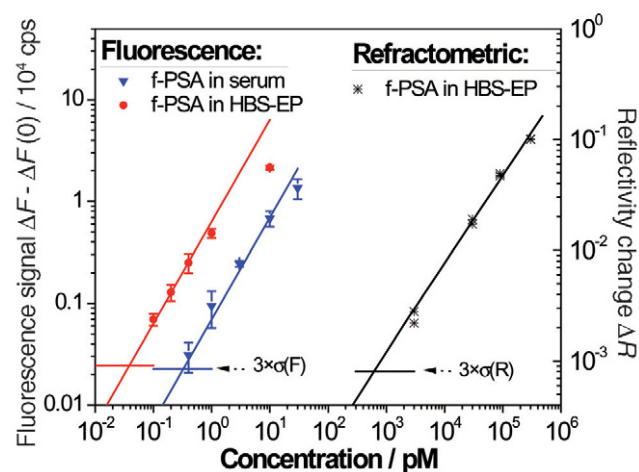


Fig. 6 Calibration curves for the direct detection of f-PSA (refractometric - stars) compared to the sandwich immunoassay-based detection with fluorescence readout for f-PSA dissolved in HBS-EP (circles) and in human serum (triangles). Lines show the linear fit and the error bars show the standard deviation.

10-minute flow of the d-Ab and 5-minute washout of the sensor surface. In comparison with the regular SPFS and dextran brush surface architecture reported by Yu *et al.*<sup>19</sup>, moderate improvement of LOD (approximately two-fold) and sample incubation time (two-fold) was achieved. In human serum, the LOD was significantly deteriorated. This effect was probably due to the non-specific interaction of the serum with the hydrogel matrix that was not observed for the dextran brush on the top of the CM5 chip (from Biacore, Sweden).

We expect that the LOD can be further improved by the optimization of the hydrogel density and thickness in order to provide faster diffusion of target analyte molecules and its binding closer to the surface where the LRSP field enhancement is stronger. In addition, compacting the capture analyte on the sensor surface through externally triggered collapse observed for "smart" gels can be used for more sensitive detection molecular binding<sup>25</sup>. For the thickness of the hydrogel matrix larger than 1  $\mu\text{m}$ , the excitation of an additional hydrogel waveguide mode was observed providing another fluorescence signal enhancement mechanism. This may provide a new, potentially even more sensitive concept for the detection of biomolecular binding events.

## The tethered bimolecular lipid membrane (tBLM)

### The basic architecture and its structural characterization

The basic architecture that contains all the essential elements of the tethered bimolecular lipid membrane and its build-up are given in Fig. 7<sup>26</sup>: On a solid support, e.g., the surface of an optical or electrical sensor transducer, the tethering system stabilizes the fluid lipid bilayer with its integrated proteins. Numerous strategies for the covalent attachment of the tethers on the different substrate materials have

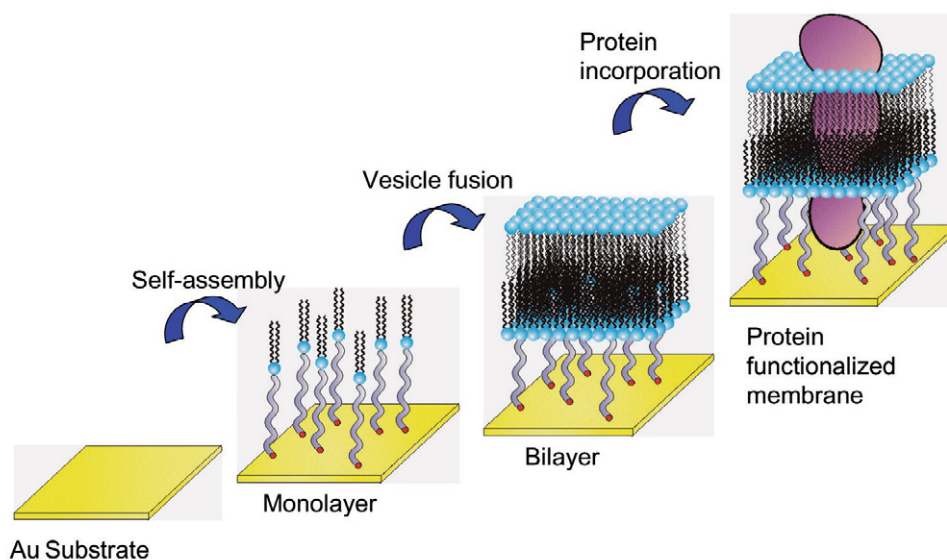


Fig. 7 The build-up of the tethered bimolecular lipid membrane (tBLM) architecture.

been worked out: the simplest one is based on a self-assembly process of end-functionalized telechelics. The resulting solid-supported tethered monolayer is completed by a fusion step whereby either liposomes of a particular lipid (mixture) or proteo-liposomes with the already integrated proteins are fused onto this monolayer resulting in the desired lipid bilayer structure<sup>27</sup>.

The experimental techniques needed to monitor the assembly and fusion steps and to characterize the obtained lipid bilayer structures include surface plasmon spectroscopy, surface plasmon fluorescence spectroscopy, vibrational spectroscopies, scanning probe microscopies, the quartz crystal microbalance, and electrical/electro-chemical techniques, like impedance spectroscopy and/or cyclic or pulsed voltammetries.

The experimental realization of this architecture has been demonstrated in our group already several years ago<sup>28</sup>. By now, we have developed a molecular tool kit for the (self-) assembly and covalent attachment of tethered monolayers onto supports of different materials classes, including:

- noble metals (Au, Ag, etc) via thiols<sup>29</sup>,
- oxide surfaces, e.g., SiO<sub>2</sub>, TiO<sub>2</sub>, etc, through silane chemistry<sup>30</sup>, and
- Al<sub>2</sub>O<sub>3</sub> by synthetic lipids derivatized with phosphonic acid groups<sup>31</sup>.

The essential properties of these solid-tethered membranes include:

- membrane fluidity with lateral diffusion coefficients of the lipid constituents of  $D \sim 1 \mu\text{m}^2/\text{sec}$ ,<sup>32</sup>
- membrane capacities of  $C = 0.5 \mu\text{F}/\text{cm}^2$ ,<sup>33</sup>
- resistivities in excess of  $R = 10 \text{ M}\Omega\text{cm}^2$ .<sup>34</sup>

In addition to the excellent performance as a model membrane these architectures coupled to the solid support demonstrated an unprecedented long term stability and robustness, another essential

prerequisite for a successful implementation in a biosensor platform. Stable performance for up to 7 months has been demonstrated. We further documented the functional incorporation of various synthetic ionophores and biological membrane proteins including, valinomycin, gramicidin, melittin, ATPases, the nicotinic acetylcholine receptor, Cytochrome c Oxidase, etc.

### Incorporation of G-protein coupled receptors (GPCRs) by *in vitro* synthesis

One of our long-term strategic goals is the development of an artificial membrane system for the investigation of complex membrane proteins, such as G-protein coupled receptors (GPCRs). The famous family of GPCRs currently constitutes the 'bottle neck' of membrane protein research: GPCR species, isolated in functional form, are practically not available. Despite the important role of GPCRs in nature, most of their regulatory, structural and functional details are still unknown. By combining materials research, surface engineering and tools from molecular biology, one hopes to be able to develop an experimental platform for the investigation of GPCRs, such as time resolved ligand binding and structure-function analysis. A recent proposal is based on the application of *in vitro* synthesis of GPCRs using the protein synthesis machinery of a cell extract in order to encompass direct incorporation of the nascent protein into a membrane mimicking structure<sup>35</sup>. This concept is schematically shown in Fig. 8. Current methods of nanotechnology provide the sensitivity and specificity together with bio-inspired synthesis providing a hydrophobic matrix with defined composition for membrane protein insertion.

With the described composite membrane platform as a 'logic gate' for membrane protein research, we intend to create a sensing device with defined molecular composition and the applicability to current analytical methods. Ligand screening of orphan GPCRs resulting in new

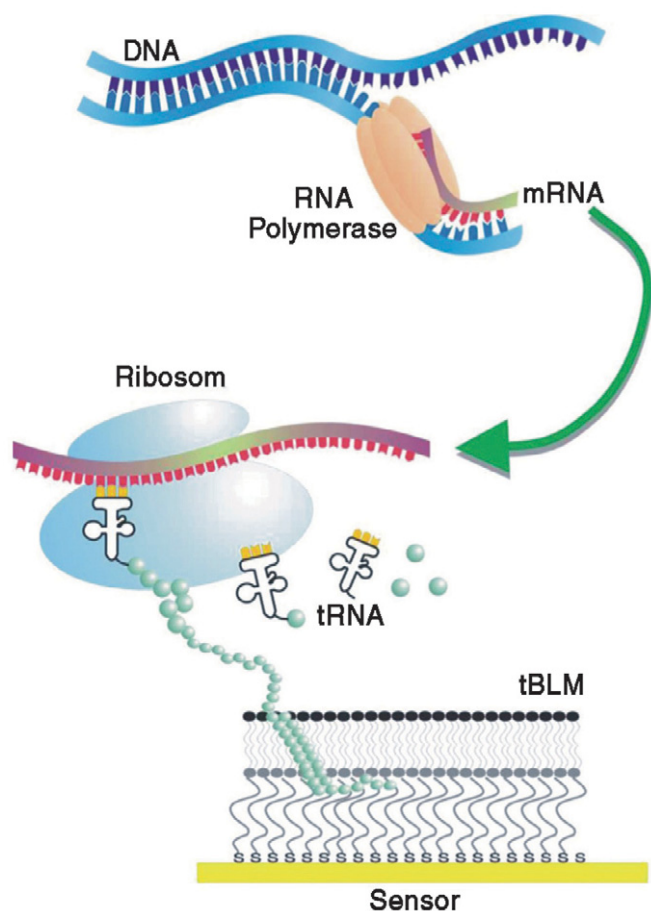


Fig. 8 The concept of cell-free expression of membrane proteins with their immediate insertion into the tethered lipid bilayer membrane: *in vitro* transcription and translation of, e.g., GPCRs.

assignments may be obtained using this platform, which significantly extend the realm of synthetic biology towards medical applications.

As a particularly challenging example for molecularly controlled functional architectures at biointerfaces we present in the following some first steps towards a biomimetic smell sensor. The sense of smell is one of the most fascinating phenomena in nature! However, olfaction, taste and hormone sensing are still among the most under-exploited areas in physiology even though the molecular players of smell, the family of olfactory receptors, have been identified already a few years ago<sup>36</sup>. The molecular discriminatory potential of the olfactory system is one of the reasons, why the sense of smell has become a major topic in fundamental research and also for technical applications.

Vision, taste and hormone sensing have been already identified as being based on the same class of receptor species<sup>37,38</sup>. Olfaction is the 'oldest' sense as it is the complex relative to chemo-reception, the most ancient and prime way of communication. With the identification of the olfactory receptors the race to apply the molecular concept of sensing at the complex level of membrane processes is on – but not much has been put on the table so far<sup>39</sup>!

Humans can sense even the faintest smells and our overall behavior is influenced by olfactory perception, consciously or unconsciously. For example, the initiation of posttraumatic shock-symptoms is related to the memory of odors. We can identify a broad spectrum of odors, but the potential of canines for extreme sensing in olfaction is by far superior. But what exactly is the difference between the olfactory system of humans and dogs? It is not the molecular characteristic of the respective odorant receptors which makes the difference in the sensing quality among canines, insect species, or humans – it is the mere cell/membrane surface area functionalized with the olfactory receptors. The specificity is defined at the molecular level of the receptor-ligand interaction itself and the sensitivity originates from the signal transduction cascade related to the receptor species.

### Signal transduction and amplification involved in olfaction

How does olfaction at the molecular level work? Each olfactory receptor species expressed in olfactory neurons specifically recognizes a set of odorants that share common molecular features<sup>40</sup>. Odorants, the ligands of the olfactory receptors, are mostly small and hydrophobic molecules; thousands of odorants have been isolated and characterized so far. Being air-borne analytes, their recognition by the receptor requires their transfer from the air to the aqueous environment of the mucosa. This is schematically (and highly oversimplified) given in Fig. 9. In addition to the (weak) partitioning of the bare odorant molecules into the aqueous phase and a passive diffusion to the receptor in the membrane, odorant binding proteins have been described as shuttle systems with relatively unspecific ligand binding capacities. They play a role in transporting the hydrophobic odorants to the cilia-structured surface of the odorant neurons carrying the odorant receptors. This is a mechanism to enhance the mere diffusion driven process of odorant transfer to the nasal mucosa, but odorant binding proteins are not involved in the signal amplification process itself<sup>41</sup>. The absence of odorant binding proteins in the standard functional assays published so far indicates that this shuttle mechanism is not crucial for the molecular interaction between receptor and odorant molecules.

How does the actual process of olfactory perception work? From the literature we know details about the concerted interaction. The first step is the translation of the binding signal into a change in the molecular structure of the receptor. As mentioned, olfactory receptors belong to the GPCR family with a structural archetype<sup>42</sup>. This has been evaluated on the basis of the structure of bacteriorhodopsin, resulting in the term of the rhodopsin-like GPCRs. The overall principle is the ligand-binding induced switching of alpha helical domains of the receptor, resulting in the activation of the eponymous G-Protein complex, consisting of three subunits: alpha, beta and gamma ( $\alpha$ ,  $\beta$ ,  $\gamma$ ). The activated G-Protein exchanges bound GDP with GTP (activation process) resulting in the dissociation of the subunits of the G-protein.



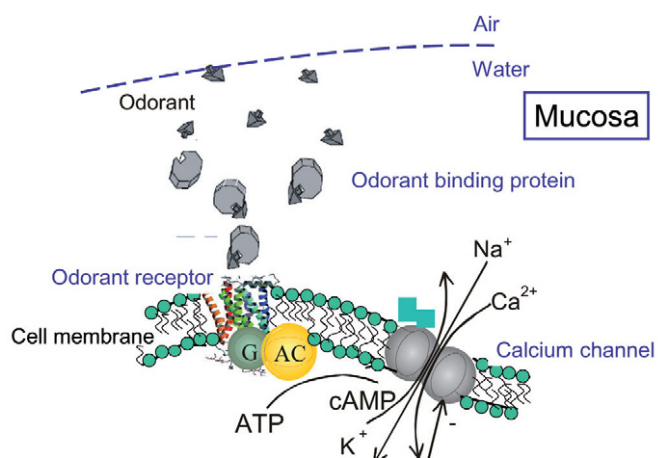


Fig. 9 Simplified scheme of the molecular steps involved in odorant reception.

In the olfactory pathway, the alpha subunit is responsible for the subsequent activation of the adenylyl cyclase. (After a certain time, the intrinsic GTPase-activity of the  $\alpha$ -subunit re-associates to the G-protein, induced by a phosphodiesterase (PDE), which lowers the cAMP concentration over time in order to regenerate the cyclic process.)

As the next steps of the complex but effective signal transduction pathway the activated adenylyl – cyclase catalyses the formation of cyclic adenosine monophosphate (cAMP) from adenosine triphosphate (ATP). The increasing concentration of cAMP is responsible for the opening of cyclic-nucleotide gated channels across the cell membrane. Those channels transport ions at rates of  $10^7$  to  $10^9$  ions per seconds resulting in a flow of ions equivalent to an electrical current on the order of 1-100 picoAmperes per channel<sup>43</sup>. Such currents are high enough to produce rapid changes in the membrane voltage, the electrical potential difference between the cell interior and exterior.

### From biological to technical solutions for olfactory sensing

The essential steps in odorant reception involve (without taking into account the de-activation strategies):

- transfer (partitioning) of odorants (hormones, biohazards, etc) from the air to the aqueous phase (mucosa) surrounding the active membrane with the embedded receptor molecules;
- passive diffusion or facilitated transport via odorant binding proteins to the odorant receptors;
- binding of the odorant to the receptor specific for that respective molecule;
- signal transduction across the membrane resulting in the detachment of the G protein from the receptor and dissociation into its  $\alpha$ - and  $\beta,\gamma$  subunits;
- binding of the  $\alpha$ - subunit of the G-protein to and activation of the membrane-bound adenylyl cyclase, resulting in a first

amplification mechanism: the binding of 1 odorant molecule results in the synthesis of ca. 1000 cAMP molecules;

- activation of a  $\text{Ca}^{++}$  channel by the cAMP resulting in a second amplification scheme by triggering the transfer of  $10^7 - 10^9$  ions per sec across the membrane through the open channel upon the binding of 1 cAMP molecule.

At the moment, it is not feasible to mimic all the molecular players involved in the biological process and use them in a technical sensor format - even though the long term perspective allows for their *in vitro* synthesis: In principle, all molecular components are known on the cDNA level, however, it has not been shown that they do assemble in bio-mimetic systems. The complete reaction scheme integrated into the underlying membrane architecture is – for the time being – too complex to be artificially built. Nevertheless, the long term goal of all corresponding research activities aims at establishing the feasibility of *in vitro* synthesis as a method for the synthesis of membrane proteins and signal transduction components to be inserted in an artificial biomimetic smell-sensor format.

As a first step into this direction, we proposed strategies that aim at reducing the complexity, however, keeping the central element of olfactory reception, i.e., the membrane bound receptor, as an essential and vital element also of the technical realization of a sensor for smells. Although essential for the smell sensor platform this strategy is also key to the development of a general biosensor platform on the basis of tethered (or supported) lipid bilayer membranes. This includes:

- the assembly of robust tethered lipid bilayer membranes on solid supports;
- the *in vitro* expression of the odorant receptor and spontaneous insertion into such model membranes;
- ultra-high sensitivity surface plasmon fluorescence detection methods with a limit of detection of c. 1000 molecules/ $\text{mm}^2$ ;
- electrical read-out capabilities for monitoring single channel opening and closing statistics;
- synthesis of mucosa-mimics based on lipid-hydrogel composites.

All of the above elements have been demonstrated in our groups in recent years. Here, we will demonstrate just a few of the key steps including the experimental evidence for the vectorial insertion of the *in vitro* synthesized odorant receptor OR5 from the rat and the first prove of its functionality by recording the IR response of the membrane protein following ligand binding.

The basic concept for the demonstration of the vectorial insertion of the receptor protein into the tethered membrane is based on the expression of the OR5 with a vesicular stomatitis virus (VSV) tag engineered by genetic manipulations to either its C – or its N-terminal end. As it is schematically sketched in Fig. 10a, one then expects a selective fluorescence signal depending on whether the tag can be identified by its corresponding monoclonal antibody or not. For this tethered membrane architecture this will be the case only if the protein is expressed properly and inserted into the tethered bilayer with a



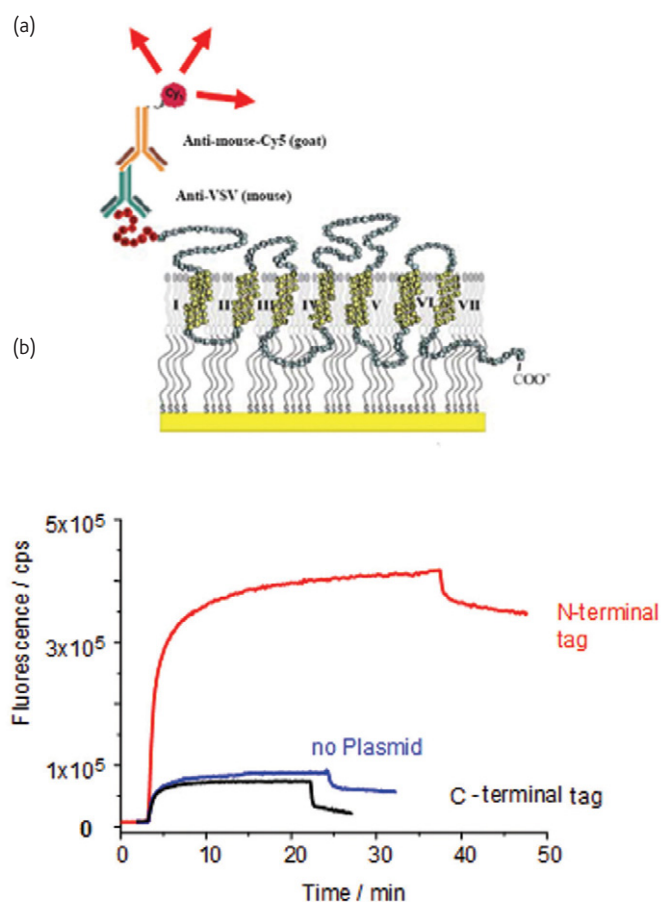


Fig. 10 (a) Schematics of the immunofluorescent analysis for the vectorial insertion of the odorant receptor OR5. The monoclonal antibody binds to the amino-terminal vesicular stomatitis virus (VSV) tag and the secondary Cy5 labelled antibody provides the specific fluorescence signal. (b) SPFS analysis for the vectorial insertion of OR5.

preferred orientation. SPFS is a uniquely sensitive tool to monitor the binding of only a few antibodies via their fluorescence label to the respective antigens immobilized by protein insertion.

This is demonstrated for the vectorial insertion of the modified OR5 in Fig. 10b. If the VSV-tag coupled to the receptor at its N-terminal end is first recognized by its primary antibody, the addition of the secondary antibody leads to a strong fluorescence signature indicating the specific orientation of the membrane inserted protein (red curve in Fig. 10b). The corresponding experiment with the VSV-tag attached to the C-terminal end results in a weak fluorescence signal (black trace in Fig. 10b) which is at the same low level as in the reference experiment in which no plasmid was given to the cell-free expression cocktail at all (blue curve), hence, no specific protein was synthesized. The weak signal that is monitored after the injection of the secondary antibody results from free proteins that are diffusing into the unstirred layer in front of the tethered membrane where they reach the evanescent tail of the surface plasmon mode, extending some 180 nm into the buffer solution (as discussed above). Upon rinsing the flow cell and

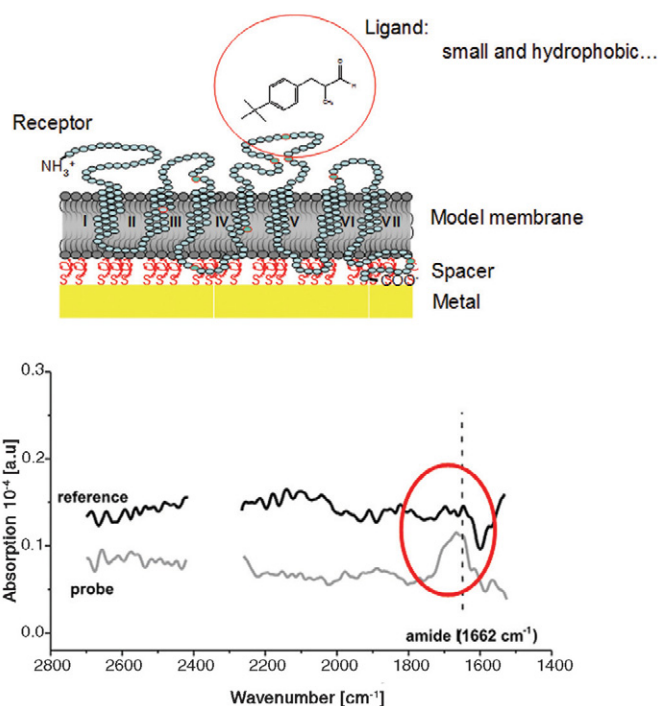


Fig. 11 (a) Schematics of the oriented insertion of the OR5 odorant receptor from the rat into a peptide-tethered lipid bilayer membrane together with the molecular structure of one of its specific ligands, lilial in this case, approaching the putative binding site in the loop region between helix 4 and 5. (b) IR spectroscopic evidence for the binding of the ligand to the membrane integral receptor as seen by the spectral changes induced in the amide I band region of the protein.

exchanging the antibody solution against free buffer this fluorescence disappears again completely.

The final piece of evidence that we present for the oriented insertion of the OR5 receptor into the tethered membrane is based on IR measurements of the interfacial lipid bilayer architecture prior to and after the binding of a ligand, the odorant lilial in our case. The schematics of the architecture and the molecular structure of the receptor in the bilayer and the ligand analyte are given in Fig. 11a. With a reference system containing no receptor protein in the membrane measured for comparison one can clearly see that the IR signature of the receptor in the amide I band region displays a change in the absorption that can be associated with the binding and of the ligand and the induced orientational changes of certain (helical) motives in the membrane protein (Fig. 11b).


## Conclusions

The presented examples for molecularly controlled functional architectures at biointerfaces demonstrate that these surface layers have reached a high degree of complexity coupled to a remarkable functionality.

In the case of the protein affinity (chip) surface the progress in recent years shows a clear path from simple 2D architectures based

on monolayers from telechelics specifically designed to allow for self-assembly at selected solid surfaces or on rather non-specifically adsorbed protein layers to the more powerful quasi-3D architectures of polymer brushes carrying a substantially higher site density to which binding of the analyte molecules from solution then leads to much higher signals. And finally, the implementation of grafted hydrogels as the ultimate in specifically tailored thickness, mechanical, temporal and chemical stability, and maximized site density, combined with an optimized access of the analyte molecules diffusing from solution to their respective binding sites within the gel show the possibilities that smart chemical concepts, molecular engineering of the matrices, and enhanced detection principles can offer.

For the tethered bimolecular lipid membranes the options for basic research using this novel model membrane platform but also for many aspects of bio-medical applications are still largely unexplored. This holds true for the mere bilayer architectures and their use for the incorporation of synthetic peptides or proteins by classical reconstitution protocols. However, this is even truer for the presented cell-free *in vitro* expression of membrane proteins. This revolutionary concept is a fundamental paradigm shift in membrane research, constituting an essential step on the way to using membranes for a wide variety of applications. The incorporation of GPCRs in general, and the presented recording of ligand binding to the odorant receptor OR5, in particular, are milestones on the way to complementing our portfolio of array technologies by the development of the

membrane chip as a molecularly controlled functional architectures at biointerfaces. The potential for basic studies is nearly unlimited however, despite its complexity it offers the stability and robustness that will allow us to implement this architecture also in biomedical applications which are so desperately in need for model systems that allow for high-throughput concepts for screening ligand targeting membrane receptors to be implemented. 

## Acknowledgement

We are grateful to a number of colleagues for stimulating discussions, in particular, to Annette Brunsen, Randolph Duran, Marcel G. Friedrich, Frank Giess, Henk Kaiser, Amal Kasry, Vincent Kirste, Ingo Köper, Joana Long, Rudolf Robelek, Robert Roskamp, Inga Vockenroth and Birgit Wiltschi.

We gratefully acknowledge the financial support of the European Commission in the Community's 6<sup>th</sup> Framework Program, the projects TRACEBACK (FOOD-CT-036300) coordinated by Tecnoalimenti and FuSyMem (FP6-2005-NEST-PATH). The contribution reflects the authors' views and the Community is not liable for any use that may be made of the information contained in this publication. Further partial support for this work was provided by the Deutsche Forschungsgemeinschaft (KN 224/18-1/2, Schwerpunktprogramm 1259 "Intelligente Hydrogele"). And finally, we are particularly thankful to financial support that came from DARPA through the MOLDICE program.

## REFERENCES

- Ratner, B. D., and Bryant, S. J., *Annu Rev Biomed Eng* (2004) **6**, 41.
- Zhang, Z., et al., *Biomaterials* (2008) **29**, 4285.
- Huang, N., et al., *Langmuir* (2002) **18**, 2280.
- Vaisocherova, H., et al., *Anal Chem* (2008) **80**, 7894.
- Cornell, B. A., et al., *Nature* (1997) **387**, 580.
- Krishna, G., et al., *Langmuir* (2003) **19**, 2294.
- Song, H., et al., *Biointerphases* (2007) **2**, 151.
- Sackmann, E., *Science* (1996) **271**, 43.
- Yu, L., et al., *BBA Biomembranes* (2009) **1788**, 333.
- Beines, P. W., et al., *Langmuir* (2007) **23**, 2231.
- Brunsen, A., et al., (2010) in preparation
- Gianneli, M., et al., *J Phys Chem* (2007) **111**, 13205.
- Raether, H., *Surface Plasmons* (1988) Springer-Verlag Berlin Heidelberg.
- Knoll, W., *Ann Rev Phys Chem* (1998) **49**, 569.
- Löfas, S., and Johansson, B., *J Chem Soc, Chem Commun* (1990) **21**, 1526.
- Liebermann, T., and Knoll, W., *Colloid Surf A* (2000) **171**, 115.
- Knoll, W., et al., In: *Handbook of Surface Plasmon Resonance*, (Eds.) Schasfoort R. B. M., and Tudos, A. J., Chpt. 9, 275-312 (2008).
- Yu, F., et al., *Anal Chem* (2003) **75**, 2610.
- Yu, F., et al., *J Am Chem Soc* (2004) **126**, 8902.
- Knoll, W., et al., In: *Topics in Fluorescence Spectroscopy, Vol 8: Radiative Decay Engineering*, (Eds.) Lakowicz, J. R., and Geddes, C. D., Ch. 10, 2005, 305.
- Sarid, D., *Phys Rev Lett* (1981) **47**, 1927.
- Sarid, D., et al., *Appl Opt* (1982) **21**, 3993.
- Kasry, A., and Knoll, W., *Appl Phys Lett* (2006) **89**, 101106.
- Wang, Y., et al., *Anal Chem* (2009) **81**, 9625.
- Huang, C. J., et al., *Proc. SPIE* (2009) **7356**, 735625.
- Knoll, W., et al., In: *Ultrathin Electrochemical Chemo- and Biosensors*, (Eds.) Wolfbeis, O. S., and Mirsky, V. M., Ch. 10, 239 (2004).
- Knoll, W., et al., *Electrochim Acta* (2008) **53**, 6680.
- Spinke, J., et al., *Biophys J* (1992) **63**, 1667.
- Schiller, S. M., et al., *Angew Chem* (2003) **42**, 208.
- Atanasov, V., et al., *Biophys J* (2005) **89**, 1780.
- Roskamp, R. F., *Tethered Bilayer Lipid Membranes auf Aluminiumoxid*, Diploma-Thesis, Mainz University, 2006
- Györfvay, E., et al. *Langmuir* (1999) **15**, 1337.
- Köper, I., et al., In: *Advances in Planar Lipid Bilayers and Liposomes*, (Ed.) Leimannova Liu, A., Ch. 2, 37, (2006)
- Knoll, W., et al., *Reviews in Molecular Biotechnology* (2000) **74**, 137.
- Robelek, R., et al., *Angew Chem Int Edit* (2007) **46**, 605.
- Buck, L. B., *Angew Chem Int Edit* (2005) **44**, 6128.
- Prinster, S. C., et al., *Pharmacol Rev* (2005) **57**, 289.
- Eilers, M., et al., *Biochemistry* (2005) **44**, 8959.
- Akimov, V., et al., *Analog Integr Circ S* (2008) **57**, 197.
- Breer, H., *Anal Bioanal Chem* (2003) **377**, 427.
- Vincent, F., et al., *Eur J Biochem* (2004) **271**, 3832.
- Floriano, W. B., et al., *Chemical Senses* (2004) **29**, 269.
- Keizer, H. M., et al., *ChemBioChem* (2007) **8**, 1246.